

A Stochastic Search for the Structures of Small Germanium Clusters and Their Anions: Enhanced Stability by Spherical Aromaticity of the Ge_{10} and Ge_{12}^{2-} Systems

Truong Ba Tai[†] and Minh Tho Nguyen^{*,†,‡}

[†]Department of Chemistry, and LMCC-Mathematical Modeling and Computational Science Center, Katholieke Universiteit Leuven, B-3001 Leuven, Belgium

[‡]Institute for Computational Science and Technology, Thu Duc, Ho Chi Minh City, Vietnam

 Supporting Information

ABSTRACT: Investigations on germanium clusters in the neutral, anionic, and dianion states Ge_n^x ($n = 2-12$ and $x = 0, -1, -2$) are performed using quantum chemical calculations with the B3LYP functional and the coupled-cluster singles and doubles [CCSD(T)] methods, in conjunction with the 6-311+G(d) basis set. An improved stochastic method is implemented for searching the low-lying isomers of clusters. Comparison of our results with previous reports on germanium clusters shows the efficiency of the search method. The Ge_8 system is presented in detail. The anionic clusters $\text{Ge}_n^{-/2-}$ are studied theoretically and systematically for the first time, and their energetics are in good agreement with available experiments. The clusters Ge_{10} , Ge_{10}^{2-} , and Ge_{12}^{2-} are, in their ground state, characterized by large highest occupied molecular orbital–lowest unoccupied molecular orbital gaps, high vertical and adiabatic detachment energies, and substantial average binding energies. The enhanced stability of these magic clusters can consistently be rationalized using the jellium electron shell model and the spherical aromatic character.

1. INTRODUCTION

Germanium (Ge) clusters have attracted much interest in part due to their possible role in surface growth processes and applications in electronic industries as alternatives to silicon-based materials. Ge thin films are in fact considered for semiconductors, and the deposition of Ge layers is generally achieved by chemical vapor deposition using germane.¹ The first experimental detection of Ge clusters containing 2–8 atoms dates back to 1954.² Subsequently, numerous experimental and theoretical investigations on the small-to-medium sized Ge_n were reported. We would refer to the most recent reports^{3–10} for the numerous earlier references. The pure Ge clusters are known to be chemically reactive and, therefore, not quite suitable as building blocks of self-assembly materials.¹¹ By using an appropriate dopant, it is however possible to modify the cluster chemical properties and thereby to design new and relevant materials. Recently, we have investigated the Cr- and Li-doped germanium clusters (Ge_nCr and Ge_nLi_m)^{12–16} and demonstrated both experimentally and theoretically that the Li-doped derivatives can actually form nanowires from units of Ge_9Li_3 .¹⁶ In small systems, the Li elements are found to attach exclusively outside the Ge cores and undergo electron transfer, and as a consequence, the Ge–Li bonds are essentially of ionic character. In Ge_{12}Li , Li can be placed inside the Ge cage, and the endohedrally doped cluster turns out to be the most stable form.¹⁷ In this context, the Ge cores of the smaller doped clusters can best be regarded as anions or polyanions Ge_n^{x-} , with $n < 12$, interacting by electrostatic forces with Li cations. Despite the fact that experimental detections of anionic clusters Ge_n^- have long been reported,^{18,19} relatively less is known about their structures and stabilities as compared with their neutral counterparts. To the

best of our knowledge, only a few theoretical studies have been devoted to the anionic clusters Ge_n^- , with n up to 8. Deutsch et al.²⁰ carried out G2 and density functional theory (DFT) calculations for the electron affinities and binding energies of Ge_n^- ($n = 2-5$). Studies of the monoanions Ge_n^- ($n = 2-6$) were performed by Xu et al.²¹ and Archibong et al.²² using the B3LYP and coupled-cluster singles and doubles [CCSD(T)] methods. In a series of theoretical investigations on the germanium clusters, both neutral and ionic Ge_n^x ($n = 5-8$ and 12 and $x = +4, +2, 0, -2, -4$), King and co-workers²³ recently proposed a geometrical analogy between the dianions Ge_n^{2-} , with $n = 5-7$, and boron hydrides $\text{B}_n\text{H}_n^{2-}$. However, this tendency does not hold true for Ge_8^{2-} where a tetrahedral structure $\text{Ge}_8^{2-}(T_d)$ is the global minimum instead of the D_{2d} structure of $\text{B}_8\text{H}_8^{2-}$.²⁴ A similar failure was also found for system containing 12 atoms in that a C_{2v} structure is the lowest-lying Ge_{12}^{2-} isomer,²⁵ whereas an icosahedron (I_h) is well established as the global minimum of $\text{B}_{12}\text{H}_{12}^{2-}$.²⁶

In view of the lack of reliable information on the anionic Ge clusters, we set out to perform a systematic study of their anionic and dianionic states. In order to evaluate the stabilities of the anions with respect to electron detachment, the corresponding neutral systems are also considered. In this study, the lower-lying isomers of clusters are initially searched for using a modified stochastic method, implemented by us,²⁷ in conjunction with reliable electronic structure methods.

Received: November 10, 2010

Published: March 07, 2011

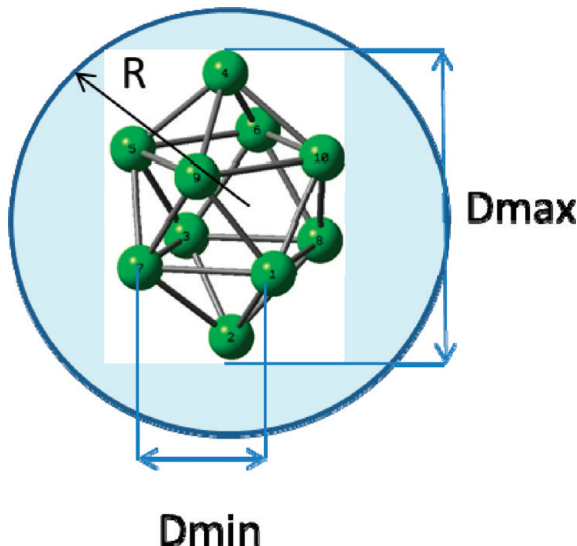


Figure 1. Control variables of the kick procedure.

2. COMPUTATIONAL METHODS

Stochastic Search for Structures. The search for the energetically lower-lying geometrical structures for large chemical compounds remains a challenge for theoretical chemists. Many search methods using various computational techniques have been proposed. For instance, the genetic algorithm-based methods have been used for searching the minima of clusters by different research groups.^{28,29} A dynamic simulated annealing method that combines molecular dynamics and DFT has widely been employed.³⁰ A ‘minimum hopping’ method used to scan the entire energy potential surface has also been put forward.³¹

Saunders³² reported a ‘random kick’ procedure for searching the low-lying isomers of compounds, which is a derivative of the stochastic search method. In this random kick procedure, each atom of an initial structure is kicked to randomly move within a sphere of radius r , and the structures so constructed will be the inputs for following geometry optimizations using electronic structure calculations. The only variable controlled here is the “moving radius” r of atoms. Although this procedure was proven to be effective for searching the global minima of compounds in recent reports, the simplicity of the procedure tends to lead to a small ratio of structures effectively converged after optimization. The structures obtained by kick in which the distance between atoms is either too short or too long are either not converged or fragmented into many smaller species upon optimization. The yield of completed optimization ranges only from 10 to 50% of the total structures generated.³³

In this work, we implement a modified stochastic searching procedure that allows the yield of completed optimization up to 90% to be attained. Similar to the original Saunders’ procedure, each of the atoms of an initial structure is kicked to randomly move within a kick radius r . However, three additional variables will be controlled to provide better structures constructed for the subsequent geometry optimization. The first variable is the distance from kicked atoms to the center of structure, called the maximum radius of molecule R (Figure 1). The next variables are the minimum distance D_{min} , and the maximum distance D_{max} between atoms. It is noted that, while the first variable is used to limit the movement of atoms and to make the kick procedure

performed more easily, the latter variables play an important role in the structure construction.

Our search for the lower-lying isomers of Ge_n is thus carried out using the improved stochastic method outlined above in conjunction with geometry optimizations by electronic structure calculations using the Gaussian 03 program package.³⁴ An input file containing the coordinate of any initial structure of Ge_n is subject for kick procedure is given in the Supporting Information. The i^{th} atom of a structure with initial coordinates (x_i, y_i, z_i) is kicked to randomly move within a sphere of radius r to new position $(x_i + dx, y_i + dy, z_i + dz)$. At this stage, three variables are controlled to obtain a new structure for a geometry optimization. First, the distance from the ‘kicked’ atom to the center of structure $\left[\{(x_i + dx)^2 + (y_i + dy)^2 + (z_i + dz)^2\}\right]^{1/2}$ must be smaller than the maximum radius R of molecule. Second, the distance between any pair of i^{th} and j^{th} atoms as defined by $\left[\{(x_i - x_j)^2 + (y_i - y_j)^2 + (z_i - z_j)^2\}\right]^{1/2}$ must be in the range of $D_{\text{min}} - D_{\text{max}}$. If both conditions are satisfied, then a new structure will then be obtained and is considered for geometry optimization using an electronic structure method. Otherwise, the structure will be rejected, and a new ‘kick’ is carried out. In general, the coordinates of the i^{th} structure obtained by the kick procedure will be used as initial coordinates for the $(i + 1)^{\text{th}}$ kick. A chart for the whole procedure is given in Scheme S1 of the Supporting Information.

A random structure for each cluster size is used as an initial coordinate for the kick procedure. Maximum radius R of molecules is chosen from 5 to 7 Å, being approximately 2–3 times as large as the bond length of the diatomic Ge_2 . The minimum distance D_{min} between two atoms is set to be 2 Å, which is slightly smaller than bond length of Ge_2 , while the maximum distance D_{max} varies within the range of 5–8 Å.

Electronic Structure Methods. The structures generated for each size are initially optimized using the popular B3LYP hybrid functional of DFT,^{35,36} along with the small 6-31G basis set. The lower-lying minima, obtained from these optimizations, characterized by harmonic vibrational frequencies at the same level, are further refined using a higher level of theory. The geometry optimization and calculation of harmonic vibrational frequencies for the located local minimum structures are further performed using the B3LYP/6-311+G(d)³⁷ level. In order to evaluate the accuracy of the calculated DFT results, single point electronic energy calculations of the smaller clusters Ge_n , with $n = 2-6$, are carried out using the CCSD(T) method,³⁸ in conjunction with the correlation consistent aug-cc-pVTZ basis set.³⁹ The molecular orbital (MO) analyses of the global minima systems are performed using the B3LYP/6-311+G(d) densities. Comparisons are made with, where appropriate, available experimental values. In addition, the stability features of clusters are considered in terms of the jellium shell model (JSM),⁴⁰ which was applied successfully on metal clusters.^{17,41}

3. RESULTS AND DISCUSSION

Efficiency of Search Method. Up to 100 structures for each size of Ge_n , in particular for $n = 6-12$, are selected using the kick procedure and initially optimized at the B3LYP/6-31G level. Due to limitation of computational resources, only the lower-lying isomers having relative energies smaller than 50 kcal/mol with respect to the global minimum are further refined using the B3LYP/6-311+G(d) level. The shapes of the lowest-lying isomers are shown in Figures 3 and 4.

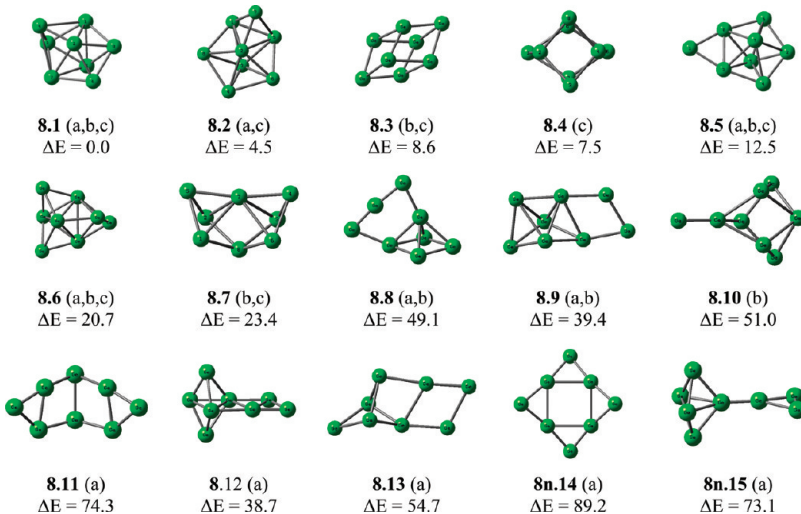


Figure 2. Shapes and relative energies (kcal/mol) of the Ge_8 isomers obtained using three different kick procedures. (a) Isomers obtained using the kick procedure without limitation of distance D ; (b) Isomers obtained using the kick procedure with $D = 2\text{--}9 \text{ \AA}$; and (c) Isomers obtained using the kick procedure with $D = 2\text{--}5 \text{ \AA}$.

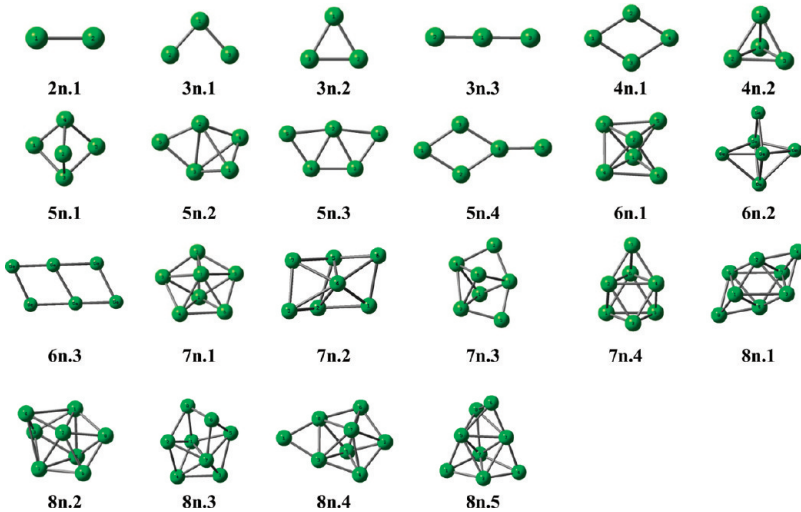


Figure 3. Shapes of the low-lying isomers Ge_n ($n = 2\text{--}8$).

Let us note that the search for structures of the small clusters Ge_n ($n \leq 7$) only results in a few novel isomers because the number of isomers of this series is rather limited, and they have already been reported. For example, for Ge_6 a new triangular prism structure is located in our search, but frequency calculations show that this structure is only a second-order saddle point having two imaginary frequencies. Therefore it is not given here. Thus, in order to evaluate the efficiency of searching method and the effect of the controlled distance D between atoms on the efficiency of the kick method, the search for Ge_8 structures is considered in more detail using three different kick procedures. All Ge_8 isomers located are given in Figure 2. In the first procedure, the kick procedure is performed without a limitation on D . With 100 structures thus obtained, the yield of completed optimization is 46%. This number rises up to 92 and 76% when Ge_8 structures are generated by kick procedures in which the distance D is limited from $D_{\min} = 2 \text{ \AA}$ to $D_{\max} = 5 \text{ \AA}$ and to $D_{\max} = 9 \text{ \AA}$, respectively. Additionally, it can be seen that when distance D is not limited, the potential energy surface scanned is larger. Thus, some less stable isomers can be located, as shown in

Figure 2, whereas some stable isomers are missed. The stable isomers with small relative energies are obtained when this distance is controlled at suitable values. Consequently, a limitation of distance D between atoms thus makes the optimization yield higher, and the structure search becomes more effective.

Similarly, a search for the low-lying isomers of the larger clusters Ge_n ($n = 9\text{--}12$) is performed, and the results are summarized Figure 4. The optimization yield varies from 80 to 90%. The local minima obtained are overall in agreement with previous reports.^{4,7}

Low-Lying Isomers of Ge_n Clusters. Characterization of the structures and stabilities of the neutral clusters Ge_n has been made. For instance, Ho and co-workers⁷ performed a search for the global minima for small clusters Ge_n ($n \leq 16$) using the combination of a genetic algorithm with an empirical tight-binding method. Wang et al.⁴ reported the low-lying isomers of medium-sized clusters ($n = 2\text{--}25$) determined by combining a genetic algorithm with a nonorthogonal tight-binding method. More recently, Zeng and co-workers⁹ searched for global minima of small-to-medium-sized germanium clusters Ge_n ($n = 12\text{--}29$) by

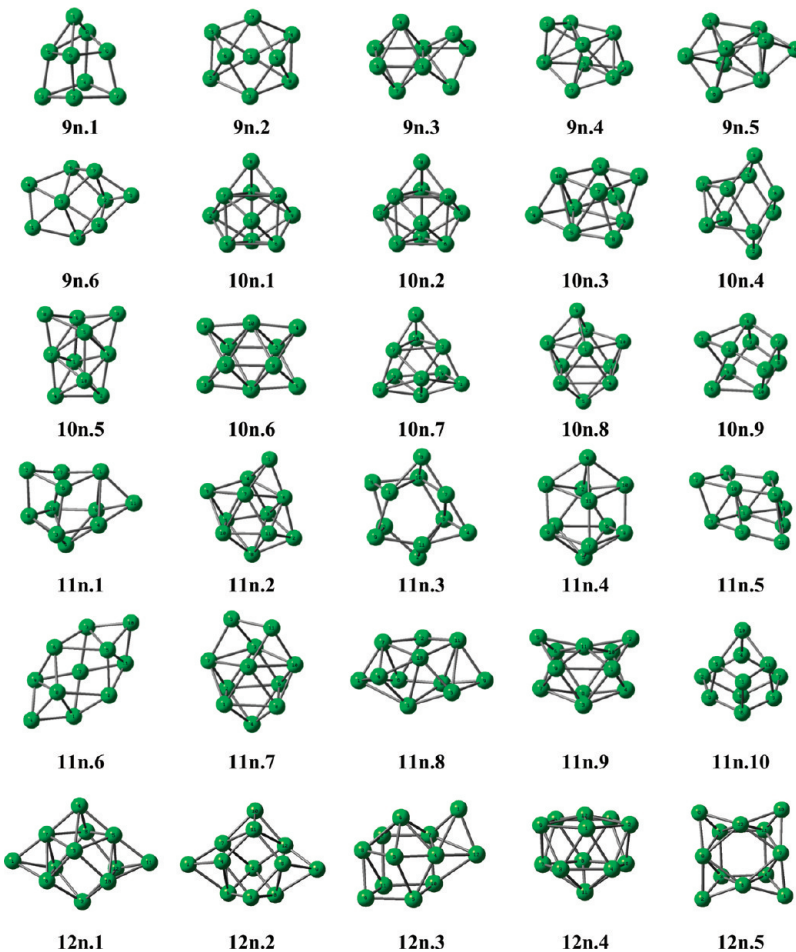


Figure 4. Shapes of the low-lying isomers Ge_n ($n = 9\text{--}12$).

using a basin-hopping algorithm coupled with the plane-wave pseudopotential density functional calculations. Although these theoretical studies have not always agreed with each other on the identity of the most stable forms in some large systems, the global minima of the small Ge clusters are now well established.

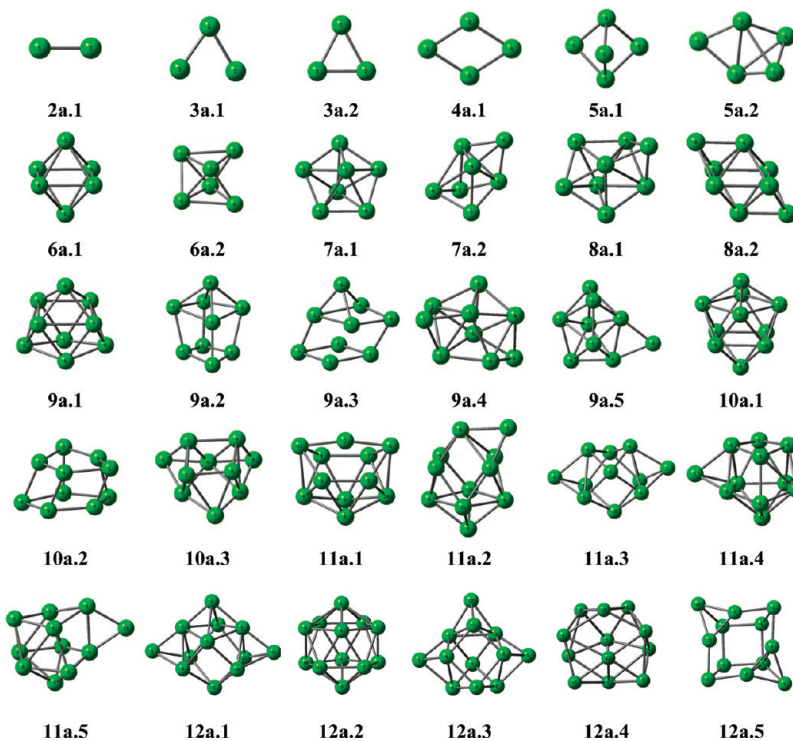
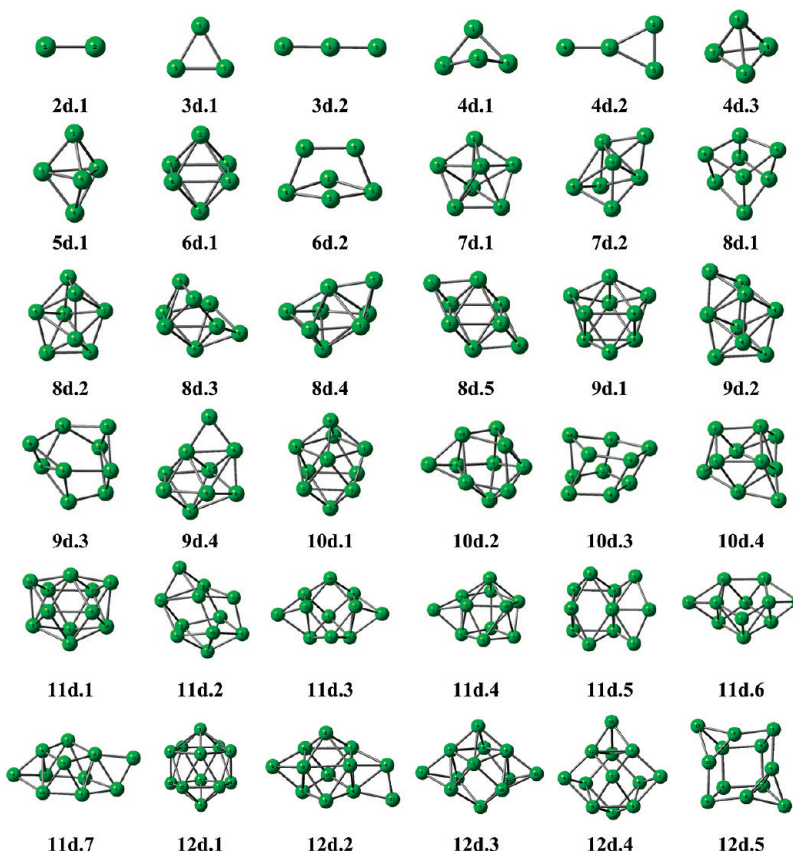
While the shapes of the low-lying isomers Ge_n^x at neutral, anionic, and dianionic states are shown in Figure 3–6, their point group, electronic state, and relative energies are given in Tables 1 and 2. In the Figures as well as in the following Discussion Section, the relative energies given are evaluated with respect to the global minimum in each isomeric system. In good agreement with earlier results,^{4,6–8} the structures **2n.1** (${}^3\Sigma_g^-$), **3n.1** ($C_{2v}, {}^1A_1$), **4n.1** ($D_{2h}, {}^1A_1'$), **5n.2** ($D_{3h}, {}^1A_1'$), **6n.1** ($C_{2v}, {}^1A_1$), and **7n.1** ($D_{5h}, {}^1A_1'$) (Figure 3) are found to be the global minima of Ge_2 , Ge_3 , Ge_4 , Ge_5 , Ge_6 , and Ge_7 , respectively. However, some high-stability isomers are also found in our search. Two structures **3n.1** and **3n.2** are almost degenerate with a negligible energy difference of 0.5 kcal/mol at the B3LYP/6-311+G(d) level. This gap slightly increases to 1.4 kcal/mol at the CCSD(T)/aug-cc-pVTZ level. Thus we prefer to assign **3n.1** as a global minimum for Ge_3 . Similarly, two structures **6n.1** and **6n.2** are found to be degenerate with relative energy of only 0.3 kcal/mol at the CCSD(T) level. At the B3LYP/6-311+G(d) + zero point energy (ZPE) level, we found that two structures **8n.1** ($C_{2v}, {}^1A_g$) and **8n.2** ($C_s, {}^1A'$) are almost degenerate. Our CCSD(T) results show a similar ordering in which **8n.1** is 1.2 kcal/mol more stable than **8n.2**. The next isomer is **8n.3** ($C_{2v}, {}^1A$), being only 3.0 kcal/mol higher in energy. Both isomers **8n.4** ($C_s, {}^1A'$) and **8n.5**

($C_1, {}^1A$) also turn out to be stable, as they are 4.8 and 10.9 kcal/mol higher in energy, respectively.

Our findings point out that **9n.1** ($C_1, {}^1A$), which is distorted from a high symmetry D_{3h} structure, is the global minimum for neutral Ge_9 (Figure 4). The following isomer is a C_{2v} structure **9n.2** with a relative energy of only 2.4 kcal/mol. Other structures are found to be less stable, being at least 12.3 kcal/mol above.

For Ge_{10} , two degenerate structures **10n.1** ($C_{3v}, {}^1A_1$) and **10n.2** ($C_1, {}^1A$), a distorted form of **10n.1**, are found with a tiny energy difference of 0.9 kcal/mol. Similar to the cases of Ge_3 and Ge_8 , this value slightly increases to 1.9 kcal/mol at the CCSD(T)/aug-cc-pVTZ level. Other forms are less stable lying at least 17.0 kcal/mol above. Structure **11n.1** ($C_1, {}^1A$) turns out to be the global minimum for the Ge_{11} system. The nearest isomer is the C_1 structure **11n.2**, which is only 3.1 kcal/mol less stable than the global minimum. For Ge_{12} , our calculated results show that the C_s structure **12n.1** is the lowest isomer. A similar structure with higher symmetry C_{2v} that is reported to be the most stable isomer at the B3LYP/6-31G(d) level²⁵ is found to have two imaginary frequencies and is much less stable with 17.8 kcal/mol higher in energy. Next isomer is the C_s structure **12n.2** with relative energy of 10.8 kcal/mol.

Low-Lying Isomers of the Monoanions Ge_n^- ($n = 2\text{--}12$). Small anionic clusters Ge_n^- ($n = 2\text{--}6$) were reported by Xu et al.²¹ and Archibong et al.²² Our calculated results concur well with the previous findings that the structures **2a.1** (${}^2\Pi_u$), **3a.1** ($C_{2v}, {}^2A_1$), **4a.1** ($D_{2h}, {}^2B_2g$), **5a.1** ($D_{3h}, {}^2A_2''$), and **6a.1** ($D_{4h}, {}^2A_{2u}$) (Figure 5) are the global minima of Ge_2^- , Ge_3^- , G_4^- , Ge_5^- , and Ge_6^- ,

Figure 5. Shapes of the low-lying isomers Ge_n^- ($n = 2-12$).Figure 6. Shapes of the low-lying isomers Ge_n^{2-} ($n = 2-12$).

respectively. Two isomers 3a.1 and 3a.2 with different electronic states are degenerate with energy difference of only 0.1 and 0.5 kcal/mol at the B3LYP/6-311+G(d) and CCSD(T)/aug-cc-pVTZ levels, respectively.

mol at the B3LYP/6-311+G(d) and CCSD(T)/aug-cc-pVTZ levels, respectively.

Table 1. Symmetry Point Group and Electronic State (PG) and Relative Energy (RE, kcal/mol) of the Lower-Lying Neutral Equilibrium Structures Ge_n ($n = 2 - 12$) Using the B3LYP/6-311+G(d) Level

isomers	PG	RE	isomers	PG	RE
2n.1	$D_{\infty h}, ^3\Sigma_g^-$	0.0	9n.5	$C_s, ^1A'$	15.7
3n.1	$C_{2v}, ^1A_1$	0.0	9n.6	$C_{1v}, ^1A$	24.0
3n.2	$D_{3h}, ^3A_1'$ (1.4) ^a	0.5	10n.1	$C_{1v}, ^1A$	0.00
3n.3	$D_{\infty h}, ^3\Sigma_g^+$	10.8	10n.2	$C_{3v}, ^1A_1$	0.9 (1.9)
4n.1	$D_{2h}, ^1A_1'$	0.0	10n.3	$C_{1v}, ^1A$	18.8
4n.2	$T_d, ^1A_{1g}$	43.6	10n.4	$C_{1v}, ^1A$	17.4
5n.1	$D_{3h}, ^1A_1'$	0.0	10n.5	$C_{2v}, ^1A_1$	25.6
5n.2	$C_{1v}, ^1A$	11.7	10n.6	$C_{2h}, ^1A_g$	31.1
5n.3	$C_{2v}, ^1A_1$	28.9	10n.7	$C_{1v}, ^1A$	17.6
5n.4	$C_{2v}, ^1A_1$	35.3	10n.8	$C_{1v}, ^1A$	17.1
6n.1	$C_{2v}, ^1A_1$	0.0	10n.9	$C_{2v}, ^1A$	17.4
6n.2	$C_s, ^1A'$ (0.3)	0.0	11n.1	$C_{1v}, ^1A$	0.0
6n.3	$C_{2v}, ^1A$	29.2	11n.2	$C_{1v}, ^1A$	3.2
7n.1	$D_{5h}, ^1A_1'$	0.0	11n.3	$C_{1v}, ^1A$	7.4
7n.2	$C_{2v}, ^1A$	21.4	11n.4	$C_{1v}, ^1A$	9.6
7n.3	$C_s, ^1A'$	29.1	11n.5	$C_{1v}, ^1A$	10.8
7n.4	$C_{3v}, ^1A_1$	31.4	11n.6	$C_{2h}, ^1A_g$	11.8
8n.1	$C_{2h}, ^1A_g$	0.0	11n.7	$C_{1v}, ^1A$	13.6
8n.2	$C_s, ^1A'$ (1.2)	0.7	11n.8	$C_{1v}, ^1A$	15.4
8n.3	$C_{2v}, ^1A$	3.0	11n.9	$C_{2v}, ^1A_1$	20.0
8n.4	$C_s, ^1A'$	4.8	11n.10	$C_s, ^1A'$	22.3
8n.5	$C_{1v}, ^1A$	10.9	12n.1	$C_s, ^1A'$	0.0
9n.1	$C_{1v}, ^1A$	0.0	12n.2	$C_s, ^1A'$	10.8
9n.2	$C_{2v}, ^1A_1$	2.4	12n.3	$C_{1v}, ^1A$	13.0
9n.3	$C_{1v}, ^1A$	12.3	12n.4	$C_{5v}, ^1A_1$	15.0
9n.4	$C_{1v}, ^1A$	14.6	12n.5	$C_{2v}, ^1A_1$	16.7

^aValues given in parentheses are obtained at the CCSD(T)/aug-cc-pVTZ//B3LYP/6-311+G(d) + ZPE level.

Following attachment of one excess electron into the lowest unoccupied molecular orbital (LUMO) of the neutral Ge_7 , the D_{5h} structure **7a.1** remains the global minimum shape for Ge_7^- . The closest isomer is the C_{1v} structure **7a.2**, that is 23.8 kcal/mol less stable than **7a.1**. The structure **8a.1**, that is formed by adding one electron to LUMO of the neutral **8n.2**, is indicated to be the lowest isomers for Ge_8^- . The next isomer is the C_{2h} structure **8a.2** with a relative energy of 2.9 kcal/mol.

A number of local minima are located for the anions Ge_9^- , Ge_{10}^- , and Ge_{11}^- . The global minimum of Ge_9^- is the C_{1v} **9a.1** that is a distortion of the D_{3h} . The structures **10a.1** (C_4) and **11a.1** (C_s) are found to be the lowest-lying isomers of Ge_{10}^- and Ge_{11}^- , respectively. Following addition of one excess electron into the neutral Ge_{12} , the C_s structure **12a.1** remains to be the lowest isomer for anion Ge_{12}^- . However, we also found that the C_{5v} **12a.2** is almost degenerate to the first with relative energy of 0.1 kcal/mol at B3LYP/6-311+G(d) level (0.7 kcal/mol at CCSD(T)/aug-cc-pVTZ level), whereas the C_s **12a.3** is the next isomer with 10.1 kcal/mol higher in energy.

Global Minima of the Dianions Ge_n^{2-} ($n = 2 - 12$). Although relevant experimental studies have not yet carried out, the

Table 2. Point Group and Electronic State (PG) and Relative Energy (RE, kcal/mol) of the Lower-Lying Anionic Equilibrium Structures Ge_n^- and Ge_n^{2-} ($n = 2 - 12$) Using the B3LYP/6-311+G(d) Level

isomers	PG	RE	isomers	PG	RE
2a.1	$D_{\infty h}, ^2\Pi_u$	0.0	2d.1	$D_{\infty h}, ^1\Sigma_g^+$	0.0
3a.1	$C_{2v}, ^2A_1$	0.0	3d.1	$D_{3h}, ^1A_1'$	0.0
3a.2	$C_{2v}, ^2B_2$	0.1 (0.5) ^a	3d.2	$D_{\infty h}, ^1\Sigma_g^+$	22.1
4a.1	$D_{2h}, ^2B_{2g}$	0.0	4d.1	$D_{2d}, ^1A_1$	0.0
5a.1	$D_{3h}, ^2A_2''$	0.0	4d.2	$C_{2v}, ^1A_1$	15.1
5a.2	$C_{1v}, ^2A$	5.0	4d.3	$T_d, ^3A_1$	20.8
6a.1	$D_{4h}, ^2A_{2u}$	0.0	5d.1	$D_{3h}, ^1A_1'$	0.0
6a.2	$C_{2v}, ^2B_2$	2.1	6d.1	$O_h, ^1A_{1g}$	0.0
7a.1	$D_{5h}, ^2A_2''$	0.0	6d.2	$C_{2v}, ^1A_1$	11.2
7a.2	$C_s, ^2A'$	23.8	7d.1	$D_{5h}, ^1A_1'$	0.0
8a.1	$C_s, ^2A'$	0.0	7d.2	$C_{1v}, ^1A$	21.2
8a.2	$C_{2h}, ^2B_u$	2.9	8d.1	$T_d, ^1A_1$	0.0
9a.1	$C_{1v}, ^2A$	0.0	8d.2	$D_{2d}, ^1A_1$	3.2
9a.2	$C_{1v}, ^2A$	12.0	8d.3	$C_{1v}, ^1A$	11.4
9a.3	$C_{1v}, ^2A$	13.6	8d.4	$C_s, ^1A'$	13.3
9a.4	$C_{1v}, ^2A$	21.6	8d.5	$C_{2v}, ^1A$	14.2
9a.5	$C_{1v}, ^2A$	25.0	9d.1	$D_{3h}, ^1A_1'$	0.0
10a.1	$C_4, ^2A$	0.0	9d.2	$C_s, ^1A'$	18.9
10a.2	$C_{1v}, ^2A$	19.2	9d.3	$C_{1v}, ^1A$	32.1
10a.3	$C_{1v}, ^2A$	25.2	9d.4	$C_{1v}, ^1A$	36.3
11a.1	$C_s, ^2A'$	0.0	10d.1	$D_{4d}, ^1A_1$	0.0
11a.2	$C_{1v}, ^2A$	1.6	10d.2	$C_{1v}, ^1A$	21.4
11a.3	$C_{2v}, ^2A_1$	2.1	10d.3	$C_{1v}, ^1A$	40.7
11a.4	$C_{1v}, ^2A$	2.3	10d.4	$C_{1v}, ^1A$	36.7
11a.5	$C_s, ^2A'$	3.3	11d.1	$C_{2v}, ^1A_1$	0.0
11a.6	$C_s, ^2A'$	12.9	11d.2	$C_{1v}, ^1A$	3.0
12a.1	$C_s, ^2A'$	0.0	11d.3	$C_s, ^1A'$	3.8
12a.2	$C_{5v}, ^2A_1$	0.1 (0.7)	11d.4	$C_{1v}, ^1A$	4.8
12a.3	$C_s, ^2A''$	10.1	11d.5	$C_{1v}, ^1A$	17.9
12a.4	$C_{1v}, ^2A$	14.5	11d.6	$C_{1v}, ^1A$	24.7
12a.5	$C_{2v}, ^2A_1$	25.4	12d.3	$C_s, ^1A'$	10.5
12d.1	$I_h, ^1A_g$	0.0	12d.4	$C_s, ^1A'$	22.9
12d.2	$C_s, ^1A'$	4.5	12d.5	$C_{2v}, ^1A_1$	36.8

^aValues given in parentheses are obtained at the CCSD(T)/aug-cc-pVTZ//B3LYP/6-311+G(d) + ZPE level.

dianions Ge_n^{2-} are of interest because their structure and stability motif are similar to those of the well-known boron hydrides $\text{B}_n\text{H}_n^{2-}$. While the symmetry point groups and relative energies of the low-lying isomers Ge_n^{2-} are tabulated in Table 2, their shapes are displayed in Figure 6.

The low-spin **2d.1** ($^1\Sigma_g^+$) is found to be the ground state for Ge_2^{2-} with a relatively large singlet-triplet gap of 25.0 kcal/mol. Following addition of two excess electrons into the high-symmetry neutral Ge_3 , the doubly degenerate singly occupied molecular orbitals (SOMOs) of the triplet **3n.2** (D_{3h}) are occupied, and the singlet **3d.1** ($D_{3h}, ^1A_1'$) becomes consequently the ground state for the dianion Ge_3^{2-} . The D_{2d} structure **4d.1**, that is analogous to the global minimum D_{2d} of boron hydride dianion $\text{B}_4\text{H}_4^{2-}$, is found to be the most stable Ge_4^{2-} isomer.

In agreement with King et al.,^{23,24} the structures **5d.1** (D_{3h}), **6d.1** (O_h), **7d.1** (D_{5h}), and **8d.1** (T_d) are calculated as the global minima for Ge_5^{2-} , Ge_6^{2-} , Ge_7^{2-} , and Ge_8^{2-} , respectively. The

Table 3. Symmetry Point Groups of Ge_n and Ge_n^{2-} ($n = 2-12$) Clusters in Comparison to the Corresponding Si_n Clusters and Boron Hydrides

Ge_n	Si_n^a	B_nH_n^b	Ge_n^{2-}	Si_n^{2-a}	$\text{B}_n\text{H}_n^{2-b}$
5n.1 (D_{3h})	Si_5 (D_{3h})	B_5H_5 (C_{4v})	5d.1 (D_{3h})	Si_5^{2-} (D_{3h})	$\text{B}_5\text{H}_5^{2-}$ (D_{3h})
6n.1 (C_{2v})	Si_6 (C_{2v})	B_6H_6 (C_{2v})	6d.1 (O_h)	Si_6^{2-} (O_h)	$\text{B}_6\text{H}_6^{2-}$ (O_h)
7n.1 (D_{5h})	Si_7 (D_{5h})	B_7H_7 (C_{3v})	7d.1 (D_{5h})	Si_7^{2-} (D_{5h})	$\text{B}_7\text{H}_7^{2-}$ (D_{5h})
8n.1 (C_{2h})	Si_8 (C_{2v})	B_8H_8 (D_{2d})	8d.1 (T_d)	Si_8^{2-} (D_{2d})	$\text{B}_8\text{H}_8^{2-}$ (D_{2d})
9n.1 (C_1)	Si_9 (C_s)	B_9H_9 (C_{4v})	9d.1 (D_{3h})	Si_9^{2-} (C_s)	$\text{B}_9\text{H}_9^{2-}$ (D_{3d})
10n.1 (C_3)	Si_{10} (C_{3v})	$\text{B}_{10}\text{H}_{10}$ (C_{3v})	10d.1 (D_{4d})	Si_{10}^{2-} (D_{4d})	$\text{B}_{10}\text{H}_{10}^{2-}$ (D_{4d})
11n.1 (C_1)	Si_{11} (C_{2v})	$\text{B}_{11}\text{H}_{11}$ (C_{2v})	11d.1 (C_{2v})	Si_{11}^{2-} (C_s)	$\text{B}_{11}\text{H}_{11}^{2-}$ (C_{2v})
12n.1 (C_s)	Si_{12} (C_s)	$\text{B}_{12}\text{H}_{12}$ (C_{2v})	12d.1 (I_h)	Si_{12}^{2-} (C_{2v})	$\text{B}_{12}\text{H}_{12}^{2-}$ (I_h)

^a Structures silicon clusters are taken from ref 45. ^b Structures for boron hydrides are taken from ref 44.

D_{2d} structure **8d.2** is the next isomer that is 3.2 kcal/mol higher in energy as compared to **8d.1**.

There is indeed an overall analogy between the global minima of Ge_n^{2-} ($n = 9-11$) and those of the isovalent $\text{B}_n\text{H}_n^{2-}$. The structure **9d.2** ($D_{3h}^{-1}\text{A}_1'$) is the global minimum for Ge_9^{2-} . Other forms are much less stable being at least 18.9 kcal/mol above the latter. Similarly, the structure **10d.1** ($D_{4d}^{-1}\text{A}_1$) turns out to be the global minimum for Ge_{10}^{2-} , while the closest C_s isomer **10d.2** is 21.4 kcal/mol higher in energy.

Our calculations point out four low-lying isomers for Ge_{11}^{2-} . Although **11d.1** ($C_{2v}^{-1}\text{A}_1$) is the global minimum, the other three structures **11d.2**, **11d.3**, and **11d.4** are located with small energy differences.

In agreement with earlier reports,^{17,42} the icosahedral form (I_h) **12d.1** is the global minimum of Ge_{12}^{2-} . Next isomer is the C_s **12d.2** with relative energy of 4.5 kcal/mol. While the C_{2v} structure (like **12d.3**) that was reported to be the most stable isomer at the B3LYP/6-31G(d) level²⁵ is only a transition state with two imaginary frequencies, the **12d.3** (C_s) is quite stable with 10.5 kcal/mol above the **12d.1**.

Wade's Rule. The Wade's rule is known as an effective electron count for predicting and interpreting the structure of boron hydrides B_nH_n and hydroborate dianions $\text{B}_n\text{H}_n^{2-}$.^{43,44} Recently, some studies on the group IVA clusters showed that a structural analogy between the boron hydrides and the isovalent group IVA clusters exists. For instance, Zetsidis found a geometrical analogy between silicon clusters Si_n and Si_n^{2-} ($n = 5-13$) and corresponding deltahedral boranes B_nH_n and $\text{B}_n\text{H}_n^{2-}$, respectively.⁴⁵ This author detected a strong analogy in their structure at the magic sizes such as Si_6 and Si_{10} . As mentioned above, for the Ge_n^x clusters ($n = 5-8$ and 12 and $x = -4, -2, 0, +2, +4$), King and co-workers^{23,24} observed a geometrical analogy between the dianions Ge_n^{2-} with $n = 5-7$ and boron hydrides $\text{B}_n\text{H}_n^{2-}$. A question of interest arises is that how far the small germanium clusters Ge_n^x at both neutral and dianion states are analogous to the corresponding boron hydrides.

The symmetry of the lowest-lying isomers of the Ge clusters considered together with those of the Si clusters and boron hydrides are given in Table 3. It can be seen that the molecular structure of the Ge_n neutrals are similar to those of the Si_n neutrals. In the dianionic state, there is also a good analogy between structures of Ge_n^{2-} and $\text{B}_n\text{H}_n^{2-}$. While the B_8H_8 dianion has a D_{2d} structure, the dianion Ge_8^{2-} is a T_d structure that is actually a higher connected point group of D_{2d} . Other features are similar between both systems. Also similar to the Si clusters, the analogy to boron hydrides appears to be more marked for Ge_{10} .

Relative Stabilities of Ge_n^x Clusters. The relative stability of the clusters considered can be probed on the basis of the second-order difference in energy (Δ^2E) and the average binding energy (BE), that are defined as follows:

$$\Delta^2E(\text{Ge}_n^x) = E(\text{Ge}_{n-1}^x) + E(\text{Ge}_{n+1}^x) - 2E(\text{Ge}_n^x) \quad (1)$$

$$\text{For the neutrals : } E_b = [nE(\text{Ge}) - E(\text{Ge}_n)]/n \quad (2)$$

$$\text{For the anions : } E_b = [(n-1)E(\text{Ge}) + E(\text{Ge}^-) - E(\text{Ge}_n^-)]/n \quad (3)$$

$$\text{For the dianions : } E_b = [(n-2)E(\text{Ge}) + 2E(\text{Ge}^-) - E(\text{Ge}_n^{2-})]/n \quad (4)$$

The Δ^2E value of a Ge_n^x is calculated as the energy difference between two dissociation processes. For example, the Δ^2E of neutrals Ge_n can be obtained from: $\text{Ge}_{n+1} \rightarrow \text{Ge}_n + \text{Ge}$, and $\text{Ge}_n \rightarrow \text{Ge}_{n-1} + \text{Ge}$. As a consequence, it reflects the relative stability of Ge_n^x as compared to that of its two immediate neighbors Ge_{n+1}^x and Ge_{n-1}^x . A high value of Δ^2E suggests that the size considered has a high relative stability as compared to its neighbors. The plots of Δ^2E displayed in Figure 7 of all systems considered reveal that the remarkably high peaks are found at $n = 10$ in all neutral, anionic, and dianionic states. This observation is consistent with the previous predictions that the Ge_{10} neutral is highly stable within the series of small Ge_n clusters. At the neutral and anionic states, the clusters $\text{Ge}_7^{0/-}$ are also stable species relative to their neighbors, whereas the dianion Ge_7^{2-} is characterized by a small value of Δ^2E .

The plots of average binding energy (E_b) showed in Figure 8 reveal similar trends for the neutrals, anions, and dianions. The E_b values thus tend to increase with the increasing size of clusters, and maximum peaks are again observed at the size of $n = 10$. It is remarkable that the binding energy of Ge_{12}^{2-} (I_h) is slightly larger as compared to that of Ge_{11}^{2-} . Consequently, Ge_{12}^{2-} is expected to be a system with enhanced stability within the series of dianion Ge_n^{2-} . Addition of one excess electron to neutrals to form anions increases the average binding energy (E_b) of anions, while dianions show lower values due to their inherent instability.

It is useful to state again that the second-order energy difference given in Figure 7 only suggests about the stability of a cluster with respect to its immediate neighbors. Thus, although both Ge_7 and Ge_{10} clusters have comparable peaks in this plot,

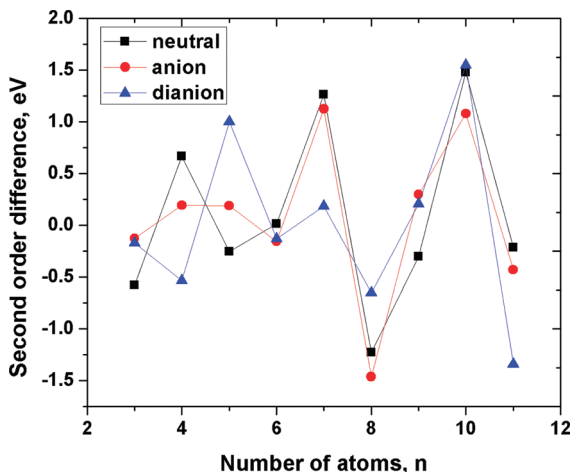


Figure 7. Second-order differences in total energies of germanium clusters Ge_n at neutral, anionic, and dianionic states using the B3LYP/6-311+G(d) level.

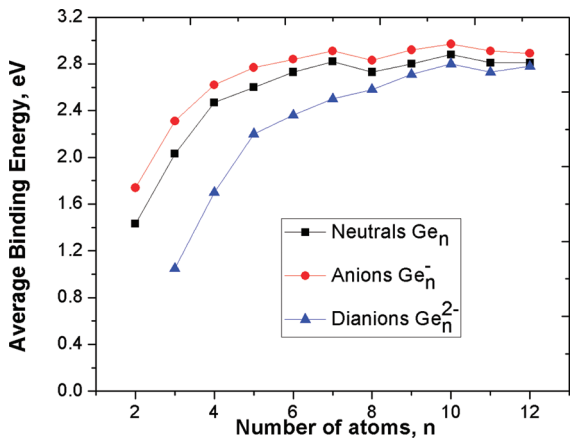


Figure 8. Average binding energies of germanium clusters Ge_n at neutral, anionic, and dianionic states using the B3LYP/6-311+G(d) level.

their relative thermodynamic stability can better be compared from the plot of binding energies illustrated in Figure 8.

Vertical Detachment Energies (VDE) and Adiabatic Detachment Energies (ADE). The values of VDE and ADE can be considered as a measure of stability of an anion with respect to electron removal. For neutrals, these actually correspond to the ionization energies (IE). The VDE corresponds to the difference in energies of the anionic and neutral states at the anion geometry. Similarly, this value of dianion Ge_n^{2-} is obtained by energy difference between the dianion and the anion with geometry of corresponding dianion. The adiabatic values are obtained from energies of the corresponding optimized structures. The VDE and ADE values of the Ge_n , Ge_n^- , and Ge_n^{2-} calculated using both B3LYP and CCSD(T) methods are given in Tables 4–6, respectively. First, it can be observed that there is a negligible difference between the B3LYP and CCSD(T) relative values for small neutrals Ge_n^x ($n = 2–7$). This difference varies in the range of 0.01–0.03 eV for VDE's and ADE's of anions. Due to limitation of computational resources, the larger clusters Ge_n^x ($n = 8–11$) are only considered using the B3LYP method, whose results are expected to deviate by ± 0.1 eV relative to the CCSD(T) results.

Table 4. Vertical Ionization Energies (VIE) of the Neutrals Ge_n ($n = 2–12$) Using Both B3LYP/6-311+G(d) and CCSD(T)/aug-cc-pVTZ Levels

neutrals Ge_n	cations Ge_n^+	VIE (eV)		
		B3LYP	CCSD(T)	exptl ^a
2n.1 (${}^3\Sigma_g^+$)	$\text{Ge}_2^+ ({}^2\Sigma_g^+)$	8.21	8.22	7.58–7.76
3n.1 (1A_1)	$\text{Ge}^+ ({}^2B_2)$	7.97	7.98	7.97–8.09
4n.1 (${}^1A_1'$)	$\text{Ge}_4^+ ({}^2B_{1u})$	7.83	7.81	7.87–7.97
5n.1 (${}^1A_1'$)	$\text{Ge}_5^+ ({}^2E')$	7.89	7.91	7.87–7.97
6n.1 (1A_1)	$\text{Ge}_6^+ ({}^2A_1)$	7.71	7.74	7.58–7.76
7n.1 (${}^1A_1'$)	$\text{Ge}_7^+ ({}^2E_2')$	7.80		7.58–7.76
8n.1 (1A_g)	$\text{Ge}_8^+ ({}^2A_u)$	6.93		6.72–6.94
9n.1 (${}^1A'$)	$\text{Ge}_9^+ ({}^2A')$	7.24		7.06–7.24
10n.1 (1A)	$\text{Ge}_{10}^+ ({}^2A)$	7.46		7.46–7.76
11n.1 (1A)	$\text{Ge}_{11}^+ ({}^2A)$	6.56		6.55–6.72
12n.1 (${}^1A'$)	$\text{Ge}_{12}^+ ({}^2A'')$	6.95		6.94–7.06

^a Experimental values are taken from ref 19.

For the neutrals, our calculated results are in good agreement with the available experimental values.¹⁹ The Ge_7 and Ge_{10} exhibit indeed high VIE values that are followed by drops of VIEs. Consequently, these neutrals are expected to be high stability, with less-stable cationic counterparts, which is consistent with previous reports.^{4,6} In the anionic state, our calculated results for small Ge_n ($n = 2–7$) at both B3LYP and CCSD(T) methods agree well with experimental values and also with previous theoretical predictions. The ADEs of Ge_2^- , Ge_3^- , and Ge_4^- determined at the CCSD(T)/aug-cc-pVTZ + ZPE level amount to 2.05, 2.19, and 2.00 eV, respectively, which can be compared to the corresponding experimental values¹⁹ of 2.035 (Ge_2^-) 2.23 (Ge_3^-), and 1.94 eV (Ge_4^-). For Ge_5^- , the ADE obtained from energy difference between the anion **5a.1** ($D_{3h} {}^2A_2''$) and the neutral **5n.1** ($D_{3h} {}^1A_1'$) is 2.20 eV, while the ADE calculated from the anion **5a.2** and neutral **5n.2** amounts to 2.49 eV. The latter is in better agreement with the experimental value of 2.51 eV. Similarly, the ADE of 2.04 eV of Ge_6^- agrees well with the experimental value of 2.06 eV, whereas the ADE of Ge_7^- is 1.94 eV by CCSD(T)/aug-cc-pVTZ is slightly larger than the available experimental value of 1.79 ± 0.06 eV.

For Ge_8^- , the ADE evaluated from the energy difference between the anion **8a.1** ($C_s {}^2A'$) and the neutral **8n.3** ($C_1 {}^1A$) is equal to 2.36 eV in good agreement with the experimental value of 2.41 eV. Although the pair C_{2h} **8n.1** and **8a3** are stable isomers at both neutral and anionic states, the corresponding ADE value of 2.10 eV obtained from them differs much from the experimental value of 2.41 eV.

Some ADE values obtained from the lowest-lying isomers of larger systems Ge_n^- ($n = 9–11$) are summarized in Table 4. While the ADE value of 2.42 eV of Ge_{11}^- (**11a.2** – $e^- \rightarrow$ **11n.2**) is in a good agreement with experiment (2.50 eV), the deviation between our calculated results and available experimental ADE values of Ge_9^- and Ge_{10}^- is considerably larger. In fact, the ADE of Ge_9^- (**9a.1** – $e^- \rightarrow$ **9n.2**) and Ge_{10}^- (**10a.1** – $e^- \rightarrow$ **10n.1**) is 2.57 and 2.21 eV, respectively, that is consistently but significantly smaller than the corresponding experimental values of 2.86 and 2.50 eV.¹⁸ Two ADE values are calculated for Ge_{12}^- , including (**12a.1** – $e^- \rightarrow$ **12n.1**) and (**12a.2** – $e^- \rightarrow$ **12n.4**). First value of 2.25 eV is in excellent agreement with the experimental value of 2.25 eV,¹⁸ the second of 2.91 eV is much higher due to less stability of the corresponding neutral **12n.4**.

Table 5. Vertical Detachment Energies (VDE) and Adiabatic Detachment Energies (ADE) of the Anions Ge_n^- ($n = 2-12$) Using B3LYP/6-311+G(d) and CCSD(T)/aug-cc-pVTZ Levels

anion	ADE (eV)					VDE (eV)		
	neutral	B3LYP	CCSD(T)	ref 22	expt. ^a	neutral	B3LYP	CCSD(T)
2a.1 ($^2\Pi_u$)	2n.1 ($^3\Sigma_g^+$)	1.94	2.05	1.95	2.035 ± 0.001	Ge_2 ($^3\Sigma_g^+$)	2.01	2.07
3a.1 (2A_1)	3n.1 (1A_1)	2.18	2.19	2.15	2.23 ± 0.01	Ge_3 (1A_1)	2.49	2.42
4a.1 ($^2B_{2g}$)	4n.1 ($^1A_1'$)	1.94	2.00	1.80	1.94	Ge_4 (1A_g)	1.96	2.02
5a.1 ($^2A_2''$)	5n.1 ($^1A_1'$)	2.20	2.30	2.10		Ge_5 ($^1A_1'$)	2.87	2.84
5a.2 (2A)	5n.2 (1A)	2.49	2.54	—	2.51	Ge_5 (1A)	3.29	3.35
6a.1 ($^2A_{2u}$)	6n.1 (1A_1)	2.01	2.04	2.01	2.06	Ge_6 (1A_1)	2.60	2.61
7a.1 ($^2A_2''$)	7n.1 ($^1A_1'$)	1.99	1.94	—	1.80	Ge_7 ($^1A_1'$)	2.30	2.30
8a.1 ($^2A'$)	8n.3 (1A)	2.36			2.41	Ge_8 ($^1A'$)	2.70	
8a.2 (2B_u)	8n.1 (1A_g)	2.10				Ge_8 ($^1A'$)	2.44	
9a.1 ($^2A'$)	9n.2 (1A_1)	2.57			2.86	Ge_9 ($^1A'$)	3.20	
10a.1 (2A_1)	10n.1 (1A)	2.21			2.50	Ge_{10} (1A_1)	3.16	
11a.1 ($^2A'$)	11n.9 (1A)	3.20				Ge_{11} ($^1A'$)	2.93	
11a.2 ($^2A'$)	11n.2 (1A)	2.42			2.50	Ge_{11} ($^1A'$)	2.83	
11a.3 ($^2A'$)	11n.1 (1A)	2.27				Ge_{11} ($^1A'$)	2.96	
12a.1 ($^2A'$)	12n.1 ($^1A'$)	2.25			2.25	Ge_{12} ($^1A'$)	2.91	
12a.2 (2A_1)	12n.4 (1A_1)	2.91				Ge_{12} (1A_1)	3.43	

^a Experimental values are taken from ref 18.**Table 6.** Vertical (VDE) and Adiabatic (ADE) Detachment Energies of the Dianions Ge_n^{2-} ($n = 2-12$) Using B3LYP/6-311+G(d) Level

dianions	ADE		VDE		
	anions	B3LYP	anions	B3LYP	
2d.1 ($^1\Sigma_g^+$)	2a.1 ($^2\Pi_u$)	-2.47	Ge_2^- ($^2\Pi_u$)	-2.46	
3d.1 ($^1A_1'$)	3a.1 (2A_1)	-2.45	Ge_3^- ($^2E'$)	-2.36	
4d.1 (1A_1)	4a.1 ($^2B_{2g}$)	-2.36	Ge_4^- (2A_1)	-1.81	
5d.1 ($^1A_1'$)	5a.1 ($^2A_2''$)	-1.56	Ge_5^- ($^2A_2''$)	-1.23	
6d.1 ($^1A_{1g}$)	6a.1 ($^2A_{2u}$)	-1.56	Ge_6^- ($^2A_{1g}$)	-1.18	
7d.1 ($^1A_1'$)	7a.1 ($^2A_2''$)	-1.60	Ge_7^- ($^2A_2''$)	-1.25	
8d.1 (1A_1)	8a.1 (C_{1a})	-0.81	Ge_8^- (2A_1)	-0.62	
9d.1 ($^1A_1'$)	9a.1 ($^2A'$)	-0.59	Ge_9^- ($^2A_2''$)	-0.45	
10d.1 (1A_1)	10a.1 (2A)	-0.39	Ge_{10}^- (2A_1)	-0.16	
11d.1 (1A_1)	11a.1 ($^2A'$)	-0.67	Ge_{11}^- (2A_1)	-0.47	
12d.1 (1A_g)	12a.2 (2A_1)	-0.03	Ge_{12}^- (2E_g)	0.27	

Most of the free dianions Ge_n^{2-} are not stable with respect to electron detachment, as indicated by their negative VDE and ADE values. The Ge_{12}^{2-} shows a positive VDE value of 0.37 eV, which lends a further support for its enhanced stability.

HOMO–LUMO Gaps. The frontier orbital energy gaps can also be regarded as a measure of kinetic stability. A large gap suggests a relatively low reactivity. The gaps of Ge_n obtained at the B3LYP/6-311+G(d) level are summarized in Table 7. Similar to the trends observed from the second order difference in energy $\Delta^2 E$ and VDE (ADE), the highest occupied molecular orbital–lowest unoccupied molecular orbital (HOMO–LUMO) gaps are found to be high at the size $n = 10$, that again points out an enhanced stability of Ge_{10}^x within the Ge_n series. As observed from BE and VDE values, the HOMO–LUMO gap of Ge_{12}^{2-} is equal to 3.0 eV, which corresponds to the highest value within the series of dianions. Although Ge_7 also has a local

Table 7. HOMO–LUMO Gaps (HLG, eV) of the Global Minima Ge_n^x ($n = 2-12, x = 0, -2$)^a

isomer	HLG	isomer	HLG
2n.1	0.81	2d.1	1.17
3n.1	2.33	3d.1	1.55
4n.1	2.35	4d.1	1.84
5n.1	3.06	5d.1	2.27
6n.1	3.02	6d.1	2.22
7n.1	2.86	7d.1	1.95
8n.1	2.27	8d.1	2.59
9n.1	2.66	9d.1	2.06
10n.1	3.03	10d.1	2.92
11n.1	2.18	11d.1	2.11
12n.1	2.84	12d.1	3.05

^a At the B3LYP/6-311+G(d) level.

maximum peak on the plot of the second-order difference (see above), its HOMO–LUMO gap of 2.8 eV is slightly smaller than that of 3.0 eV for Ge_{10} .

Enhanced Stability and JSM. Finding a consistent rationalization for stability of clusters is always an important goal. In previous reports, stability of the Ge_n clusters can be interpreted using a simple shell model which assumes that each Ge atom distributes two valence electrons from its p-subshell into the electron shell configuration of system. As a result, Ge_{10} contains 20 valence electrons and becomes a thermodynamically stable species due to a possession of a filled electron shell configuration, similar to the situation of alkali metals.

In order to probe the features related to the stability of Ge_n clusters, we re-examine their MO pictures under the viewpoint of the JSM,⁴⁰ which is applied successfully to interpret the stability motif of different types of atomic clusters. According to this rather simple model in which the valence electrons are assumed to be freely itinerant in a simple mean-field potential formed by

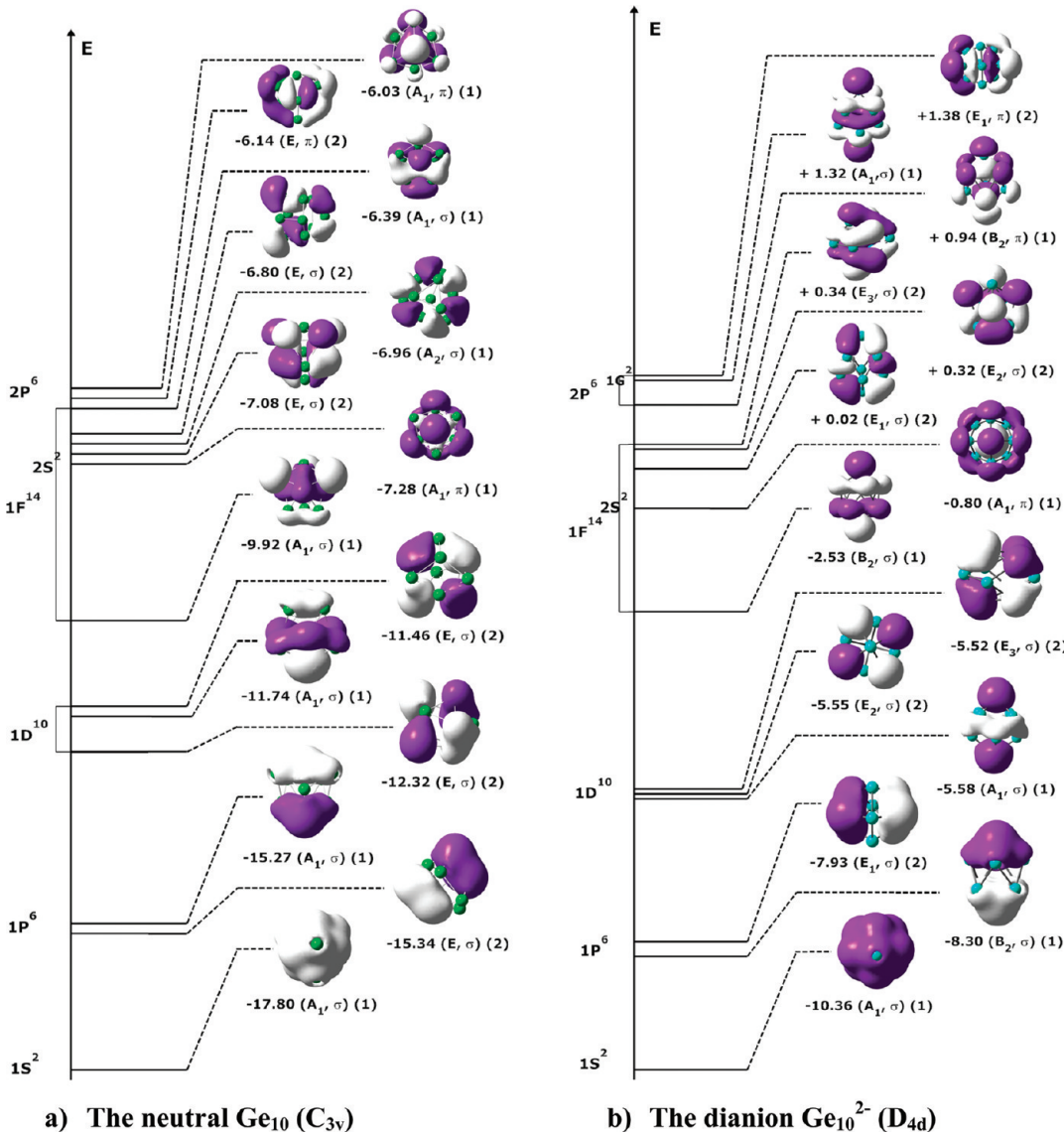


Figure 9. Energy levels and orbitals of the Ge_{10} (C_{3v}) and Ge_{10}^{2-} (D_{4d}) using the B3LYP/6-311+G(d) level.

the nuclei of atoms, the valence electrons fill the spherical orbitals of a system according to the pattern of $[1\text{S}^2 1\text{P}^6 1\text{D}^{10} 2\text{S}^2 1\text{F}^{14} - 2\text{P}^6 1\text{G}^{18} 2\text{D}^{10} \dots]$, etc. As a consequence, the number of electrons of 8, 20, 34, 40, 56, and 68, etc. are proposed as the magic numbers that correspond to the closed shell electrons. We should note that the observed number of electrons of a simple JSM is predicted on the basis of a spherical background. Thus, these magic numbers can be changed due to a lowering of the molecular symmetry.

As for a typical case, let us show the MO pictures of Ge_{10} that features an enhanced stability in the neutral state. Each Ge atom is expected to contribute its four valence electrons to the electron shell configuration of the system. The Ge_{10} cluster thus contains 40 valence electrons with an orbital configuration of $[1\text{a}_1^2 1\text{e}_4^4 - 2\text{a}_1^2 2\text{e}^4 3\text{a}_1^2 3\text{e}^4 4\text{a}_1^4 4\text{e}^4 1\text{a}_2^2 5\text{e}^4 5\text{a}_1^2 6\text{e}^4 6\text{a}_1^2]$ that can be arranged into the model energy ordering of $[1\text{S}^2 2\text{P}^6 2\text{S}^2 1\text{D}^{10} 1\text{F}^{14} 2\text{P}^6]$ (Figure 9). While the HOMO of the Ge_{10} is a p-orbital, its LUMO is a g-orbital, belongs to the model G-subshell.

Due to a lowering from a spherical background to the C_{3v} point group symmetry, the model subshells are split into different

energy levels. However, the resulting energy ordering of Ge_{10} is consistent with the electron shell configuration of 40 electrons of JSM. Overall, the Ge_{10} is a magic size within the Ge_n series.

Adding two excess electrons into the HOMO of the neutral Ge_{10} leads to an unstable system with open electronic shell configuration. However, due to a distortion from the spherical symmetry to D_{4d} symmetry, the model G-subshell of Ge_{10}^{2-} is split into P-subshells (Figure 9b). The valence electrons of the Ge_{10}^{2-} are thus composed of an orbital configuration of $[1\text{a}_1^2 1\text{b}_2^2 1\text{e}_1^4 2\text{a}_1^2 1\text{e}_2^4 1\text{e}_3^4 - 2\text{b}_2^2 3\text{a}_1^2 2\text{e}_1^4 2\text{e}_2^4 2\text{e}_3^4 3\text{b}_2^2 4\text{a}_1^2 3\text{e}_1^4]$, which corresponds to the model energy ordering of $[1\text{S}^2 1\text{P}^6 1\text{D}^{10} 2\text{S}^2 1\text{F}^{14} 2\text{P}^4 1\text{G}^2 2\text{P}^2]$. Its HOMO is the third orbital of 2P-subshell, while its LUMO belongs to a G-subshell. This gives rise to a consequence that Ge_{10}^{2-} possesses a closed shell configuration and thereby a higher stability, as compared to other Ge_n^{2-} dianions.

The enhanced stability of the icosahedral Ge_{12}^{2-} (I_h) is even more interesting. The Ge_{12}^{2-} 12d.1 contains thus 50 valence electrons that are arranged into an energy ordering as $[1\text{S}^2 1\text{P}^6 1\text{D}^{10} 1\text{F}^6 2\text{S}^2 1\text{F}^8 2\text{P}^6 1\text{G}^{10}]$ (Figure 10). Similar to systems containing 50 valence electrons reported previously, including

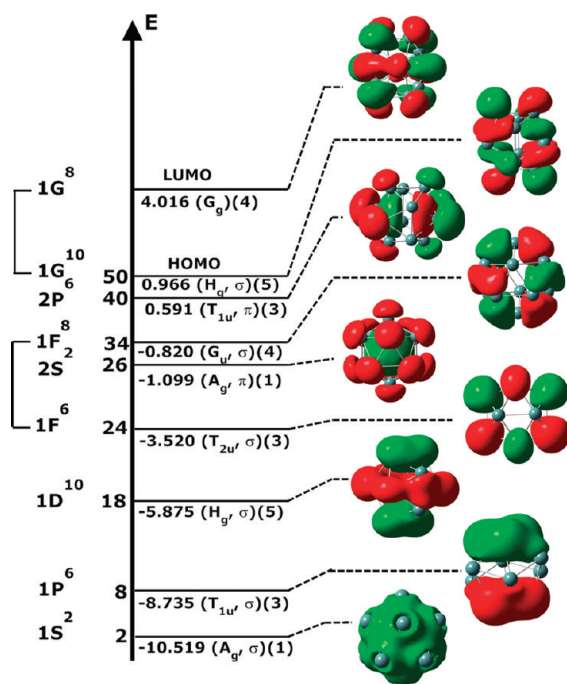


Figure 10. Energy levels and orbitals of the Ge_{12}^{2-} (I_h) using the B3LYP/6-311+G(d) level.

$\text{Pb}_{12}\text{Al}^+$,⁴⁶ Ge_{12}M^x ($\text{M} = \text{Li}, \text{Na}, \text{Be}, \text{Mg}, \text{B}, \text{and Al}$),¹⁷ a splitting of the $l = 4$ shell (G-shell) in the icosahedral 12d.1 (I_h) occurs under the crystal field effects.⁴⁷ This splitting of G-shell consequently results in a large energy gap of 3.0 eV between the frontier orbitals that ultimately leads to its high stability.

Spherical Aromaticity. Aromaticity is usually considered as one of the important measures to probe the thermodynamic stability of chemical compounds. While the Hückel rule of $(4n + 2)$ electrons is popularly applied to determine the aromatic character of planar structures, the I_h symmetrical fullerenes were reported to have spherical aromaticity through the $2(N + 1)^2$ rule, that was recently proposed by Hirsch et al.⁴⁸ The π -electron system of these species can approximately be considered as a spherical electron gas, which surrounds the surface of a sphere. The wave functions of this electron gas can be characterized by the angular momentum quantum numbers ($l = 0, 1, 2, 3, \dots$), that are comparable to the atomic s, p, d, f, ... orbitals. According to the classical Pauli principle, if a system with $2(N + 1)^2$ π -electrons fully fills all π -shells, then it then exhibits an aromatic character.

The MO picture of Ge_{10} (Figure 9a) reveals two orbital sets: While the first contains the σ -type MOs of 1S, 1P, 1D, and 1F, that are occupied by 32 σ -electrons, the second set includes the MOs of 2S (A_1, π) and 2P (E, π and A_1, π), that are thus occupied by 8 valence π -electrons. Consequently, the Ge_{10} system is characterized by eight π -electrons, that make it spherically aromatic, which is consistent with the $2(N + 1)^2$ rule.

Similar systems of eight valence π -electrons are also found for the global minima Ge_{10}^{2-} (D_{4d}) and Ge_{12}^{2-} (I_h) (Figures 9b and 10, respectively) in which each includes two π -electrons belonging to the 2S-subshell and six π -electrons belonging to the 2P-subshell. As a consequence, these dianions Ge_{10}^{2-} and Ge_{12}^{2-} possess an aromatic character that is in line with their enhanced thermodynamic stability. Ge_{10} is found to have an enhanced stability, in good agreement with previous studies. Wang et al.⁴ showed a maximum peak at Ge_{10} in their plot of fragmentation

energies, while the maximum ionization potential of the Ge_n clusters was found at $n = 10$.¹⁰ Thus, the spherical aromaticity is proposed to evaluate the aromaticity of the fullerene-like structures and is not applied to structures like Ge_7 . The stability of Ge_7 is not due to the effect of spherical aromaticity.

4. CONCLUDING REMARKS

In this theoretical study, we carry out a search for the energetically lower-lying isomers of small germanium clusters and the anions and dianions, Ge_n^x with $n = 2 - 12$ and $x = 0, -1, -2$ using a stochastic method. An improved search method for structures is implemented, and the obtained results are compared to previous reports. Using the new procedure with additional control parameters, optimization yield raises up 90%, and the larger number of isomers located shows the efficiency of the procedure. The structures of global minima Ge_n^x ($x = 0, -2$) are found to be analogous to those of boron hydrides B_nH_n^x . The negatively charged clusters Ge_n^{-2-} are systematically characterized, and the energetic results obtained using both B3LYP and CCSD(T) methods are in good agreement with available experimental values and also point out some disagreements. Calculated results show that the Ge_{10}^x clusters, in neutral and dianionic states, and Ge_{12}^{2-} clusters are the magic species with large HOMO–LUMO gaps, high VDE and ADE values, and average binding energies. The enhanced stability of Ge_{10} , Ge_{10}^{2-} , and Ge_{12}^{2-} can consistently be rationalized by using the jellium electron shell model and their high spherically aromatic character.

■ ASSOCIATED CONTENT

S Supporting Information. Tables list the total electronic energies, zero-point energies of the low-lying isomers. Figures display all isomers located for the Ge_n clusters. This material is available free of charge via the Internet at <http://pubs.acs.org>.

■ AUTHOR INFORMATION

Corresponding Author

*E-mail: minh.nguyen@chem.kuleuven.be.

■ ACKNOWLEDGMENT

The authors are indebted to the K.U. Leuven Research Council for continuing support (GOA, IDO, and IUAP programs). T.B.T. thanks the Arenberg Doctoral School for a scholarship. M.T.N. thanks the ICST of Ho Chi Minh City for supporting his stays in Vietnam.

■ REFERENCES

- Li, C.; John, S.; Banerjee, S. *J. Electron. Mater.* **1995**, *24*, 875.
- Kohl, V. G. *Z. Naturforsch.* **1954**, *9A*, 913.
- Kikuchi, E.; Ishii, S.; Ohno, K. *Phys. Rev. B: Condens. Matter Mater. Phys.* **2006**, *74*, 195410.
- Wang, J.; Han, J. G. *J. Chem. Phys.* **2005**, *123*, 244303.
- Li, B. X.; Cao, P. L. *Phys. Rev. B: Condens. Matter Mater. Phys.* **2000**, *62*, 15788.
- Bandyopadhyay, D.; Sen, P. *J. Phys. Chem. A* **2010**, *114*, 1835.
- Shvartsburg, A. A.; Liu, B.; Lu, Z. Y.; Wang, C. Z.; Jarrold, M. F.; Ho, K. M. *Phys. Rev. Lett.* **1999**, *83*, 2167.
- Wang, J.; Wang, G.; Zhao, J. *Phys. Rev. B: Condens. Matter Mater. Phys.* **2001**, *64*, 205411.

- (9) (a) Yoo, S.; Zeng, X. C. *J. Chem. Phys.* **2006**, *124*, 184309. (b) Bulusu, S.; Yoo, S.; Zeng, Z. C. *J. Chem. Phys.* **2005**, *122*, 164305.
- (10) Yoshida, S.; Fuke, K. *J. Chem. Phys.* **1999**, *111*, 3880.
- (11) Jarrold, M. F.; Bower, J. E. *J. Chem. Phys.* **1992**, *96*, 9180.
- (12) Gopakumar, G.; Lievens, P.; Nguyen, M. T. *J. Chem. Phys.* **2006**, *124*, 214312.
- (13) Gopakumar, G.; Lievens, P.; Nguyen, M. T. *J. Phys. Chem. A* **2007**, *111*, 4355.
- (14) Hou, X. J.; Gopakumar, G.; Lievens, P.; Nguyen, M. T. *J. Phys. Chem. A* **2007**, *111*, 13544.
- (15) Gopakumar, G.; Ngan, V. T.; Lievens, P.; Nguyen, M. T. *J. Phys. Chem. A* **2008**, *112*, 12187.
- (16) Gopakumar, G.; Wang, X.; Lin, L.; De Haeck, J.; Lievens, P.; Nguyen, M. T. *J. Phys. Chem. C* **2009**, *113*, 10856.
- (17) (a) Tai, T. B.; Nguyen, M. T. *Chem. Phys. Lett.* **2010**, *492*, 290. (b) Holtz, T.; Veldeman, N.; Vespremi, T.; Lievens, P.; Nguyen, M. T. *Chem. Phys. Lett.* **2009**, *469*, 304.
- (18) (a) Burton, G. R.; Xu, C.; Arnold, C. C.; Neumark, D. M. *J. Chem. Phys.* **1996**, *104*, 2757. (b) Burton, G. R.; Xu, C.; Neumark, D. M. *Surf. Rev. Lett.* **1996**, *3*, 383.
- (19) Yoshida, S.; Fuke, K. *J. Chem. Phys.* **1999**, *111*, 3880.
- (20) Deutsch, P. W.; Curtiss, L. A.; Blaudeau, J. P. *Chem. Phys. Lett.* **1997**, *270*, 413.
- (21) Xu, W.; Zhao, Y.; Li, Q.; Xie, Y.; Schaefer, H. F., III. *Mol. Phys.* **2004**, *102*, 579.
- (22) Archibong, E.; St-Amant, A. *J. Chem. Phys.* **1998**, *109*, 962.
- (23) King, R. B.; Dumitrescu, I. S.; Kun, A. *J. Chem. Soc., Dalton Trans.* **2002**, 3999.
- (24) King, R. B.; Dumitrescu, I. S.; Lupon, A. *J. Chem. Soc., Dalton Trans.* **2005**, 1858.
- (25) King, R. B.; Dumitrescu, I. S.; Uta, M. M. *J. Chem. Soc., Dalton Trans.* **2007**, 364.
- (26) Nguyen, M. T.; Matus, M. H.; Dixon, D. A. *Inorg. Chem.* **2007**, *46*, 7561.
- (27) Tai, T. B.; Nguyen, M. T. *Kwant-Kick*: A program for searching cluster structures using a stochastic approach, K. U. Leuven (2010)
- (28) Zhao, J.; Xie, R. *J. Comput. Theor. Nanosci.* **2004**, *1*, 117.
- (29) Alexandrova, A. N.; Boldyrev, A. I. *J. Chem. Theory Comput.* **2005**, *1*, 566.
- (30) Car, R.; Parrinello, M. *Phys. Rev. Lett.* **1985**, *55*, 2471.
- (31) Goedecker, S. *J. Chem. Phys.* **2004**, *120*, 9911.
- (32) Saunders, M. *J. Comput. Chem.* **2003**, *25*, 621.
- (33) Bera, P. P.; Sattelmeyer, K. W.; Saunders, M.; Schaefer, H. F., III; Schleyer, P. v. R. *H. J. Phys. Chem. A* **2006**, *110*, 4287.
- (34) Frisch, M. J.; Trucks, G. W.; Schlegel, H. B.; Scuseria, G. E.; Robb, M. A.; Cheeseman, J. R.; Montgomery, Jr., J. A.; Vreven, T.; Kudin, K. N.; Burant, J. C.; Millam, J. M.; Iyengar, S. S.; Tomasi, J.; Barone, V.; Mennucci, B.; Cossi, M.; Scalmani, G.; Rega, N.; Petersson, G. A.; Nakatsuji, H.; Hada, M.; Ehara, M.; Toyota, K.; Fukuda, R.; Hasegawa, J.; Ishida, M.; Nakajima, T.; Honda, Y.; Kitao, O.; Nakai, H.; Klene, M.; Li, X.; Knox, J. E.; Hratchian, H. P.; Cross, J. B.; Bakken, V.; Adamo, C.; Jaramillo, J.; Gomperts, R.; Stratmann, R. E.; Yazyev, O.; Austin, A. J.; Cammi, R.; Pomelli, C.; Ochterski, J. W.; Ayala, P. Y.; Morokuma, K.; Voth, G. A.; Salvador, P.; Dannenberg, J. J.; Zakrzewski, V. G.; Dapprich, S.; Daniels, A. D.; Strain, M. C.; Farkas, O.; Malick, D. K.; Rabuck, A. D.; Raghavachari, K.; Foresman, J. B.; Ortiz, J. V.; Cui, Q.; Baboul, A. G.; Clifford, S.; Cioslowski, J.; Stefanov, B. B.; Liu, G.; Liashenko, A.; Piskorz, P.; Komaromi, I.; Martin, R. L.; Fox, D. J.; Keith, T.; Al-Laham, M. A.; Peng, C. Y.; Nanayakkara, A.; Challacombe, M.; Gill, P. M. W.; Johnson, B.; Chen, W.; Wong, M. W.; Gonzalez, C.; and Pople, J. A. *Gaussian 03*, revision C.01; Gaussian, Inc.: Wallingford, CT, 2004.
- (35) Lee, C.; Yang, W.; Parr, R. G. *Phys. Rev. B: Condens. Matter Mater. Phys.* **1988**, *37*, 785.
- (36) Rassolov, V. A.; Ratner, M. A.; Pople, J. A.; Redfern, P. C.; Curtiss, L. A. *J. Comput. Chem.* **2001**, *22*, 976.
- (37) Binning, R. C.; Curtiss, L. A. *J. Comput. Chem.* **1990**, *11*, 1206.
- (38) Pople, J. A.; Head-Gordon, M.; Raghavachari, K. *J. Chem. Phys.* **1987**, *87*, 5968.
- (39) Wilson, A. K.; Woon, D. E.; Perterson, K. A.; Dunning, T. H. *J. Chem. Phys.* **1999**, *110*, 7667.
- (40) Brack, M. *Rev. Mod. Phys.* **1993**, *65*, 677.
- (41) (a) Tai, T. B.; Nhat, P. V.; Nguyen, M. T. *Phys. Chem. Chem. Phys.* **2010**, *12*, 11477. (b) Tai, T. B.; Nguyen, M. T. *Chem. Phys. Lett.* **2010**, *489*, 75. (c) Holtz, T.; Veldeman, N.; De Haeck, J.; Vespremi, T.; Lievens, P.; Nguyen, M. T. *Chem.—Eur. J.* **2009**, *15*, 3970.
- (42) Shao, N.; Bulusu, S.; Zeng, X. C. *J. Chem. Phys.* **2008**, *128*, 154326.
- (43) Kalvoda, S.; Paulus, B.; Dolg, M.; Stoll, H.; Werner, H. *J. Phys. Chem. Chem. Phys.* **2001**, *3*, 514.
- (44) McKee, M. L.; Wang, Z. X.; Schleyer, P. v. R. *J. Am. Chem. Soc.* **2000**, *122*, 4781.
- (45) Zdetis, A. D. *J. Chem. Phys.* **2007**, *127*, 244308.
- (46) Neuikermans, Janssens, K.; Chen, Z. F.; Silverans, R. E.; Schleyer, P. v. R.; Lievens, P. *Phys. Rev. Lett.* **2004**, *92*, 163401.
- (47) Schriver, K. E.; Persson, J. L.; Honea, E. C.; Whetten, R. L. *Phys. Rev. Lett.* **1990**, *64*, 2539.
- (48) Hirsch, A.; Chen, Z.; Jiao, H. *Angew. Chem., Int. Ed.* **2000**, *39*, 3915.